Simultaneous Localization and Mapping Using a Novel Dual Quaternion Particle Filter

Kailai Li, **Gerhard Kurz**, **Lukas Bernreiter** and **Uwe D. Hanebeck**
Intelligent Sensor-Actuator-Systems Laboratory (ISAS)
Institute for Anthropomatics and Robotics
Karlsruhe Institute of Technology (KIT), Germany
kailai.li@kit.edu, gehard.kurz@kit.edu, lukas.bernreiter@student.kit.edu, uwe.hanebeck@ieee.org

***Abstract*—In this paper, we present a novel approach to perform simultaneous localization and mapping (SLAM) for planar motions based on stochastic filtering with dual quaternion particles using low-cost range and gyro sensor data. Here, $SE(2)$ states are represented by unit dual quaternions and further get stochastically modeled by a distribution from directional statistics such that particles can be generated by random sampling. To build the full SLAM system, a novel dual quaternion particle filter based on Rao–Blackwellization is proposed for the tracking block, which is further integrated with an occupancy grid mapping block. Unlike previously proposed filtering approaches, our method can perform tracking in the presence of multi-modal noise in unknown environments while giving reasonable mapping results. The approach is further evaluated using a walking robot with on-board ultrasonic sensors and an IMU sensor navigating in an unknown environment in both simulated and real-world scenarios.**

***Keywords*—simultaneous localization and mapping, stochastic filtering, directional statistics, Rao–Blackwellized particle filtering, low-cost range and gyro sensors**

I. Introduction

Simultaneous Localization and Mapping denotes the technique of constructing or updating a map of unknown surroundings while at the same time tracking an agent's location. It plays a key role in a variety of applications such as extended object tracking [1], autonomous driving [2] and robotic perception [3], localization [4] as well as navigation [5] in unknown environments. Over recent years, an extensive number of approaches have been proposed to solve this problem, among which the stochastic methods are most popular. For instance, the tracking problems are typically solved by some stochastic filtering approaches, such as the well-known Kalman Filter (KF), Extended Kalman Filter (EKF), Unscented Kalman Filter (UKF) [6] or the Particle Filter (PF) [7]. However, the mapping technique normally depends on the application scenario and the employed sensors. For example, in autonomous driving tasks it is always appealing to maintain a sufficiently detailed map where only the interested object features should be dynamically perceived. In some visual-based perception applications where dense reconstruction is required, some numerical approaches should be applied and techniques such as bundle adjustment should be used to enforce a globally consistent map. In this paper, we focus on a specific application scenario where simultaneous robotic localization and mapping is performed based on some low-cost sensors, such as ultrasonic and gyro sensors, whose measurement performance may suffer from high noise level. The following issues can make solving such a SLAM problem challenging.

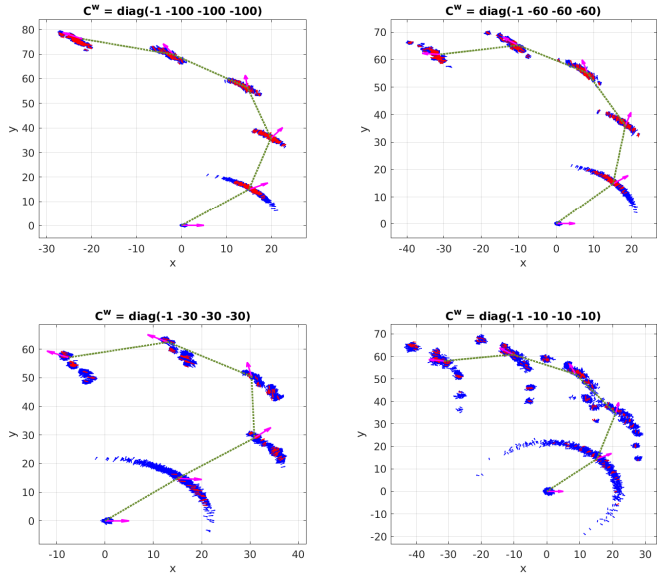

Figure 1: Dual quaternion particles of $SE(2)$ states propagating through system dynamics of different noise levels and getting updated based on importance sampling with simulated likelihoods. The simulation is given by a single run with 1000 particles.

First, the planar rigid body motions mathematically belong to the *Special Euclidean Group* $SE(2)$, which incorporates both orientation and position and have a highly nonlinear structure due to the underlying manifold. There has been continuing effort in adapting the tracking problem from the nonlinear manifold to an approximated linearized local domain, e.g., with EKF and UKF. However, the linearization operations in these tracking methods have typically the assumption of slow motions as well as low noise level and distributions used in conventional Kalman filter family lack probabilistic interpretation of the nonlinear manifold as well as the correlation between orientation and position. For handling these issues, dual quaternions can be used to represent $SE(2)$ states due to their advantages compared to other representation methods such as better numerical stability (compared with homogeneous transformation matrix), less ambiguity (compared to Euler angles where a gimbal lock can occur). Moreover, they can represent the orientation and position simultaneously in the same domain. In order to model uncertain dual quaternions, some specific distributions from the field of directional statistics are proposed, e.g., the Projected-Gaussian Distribution (PGD) [8] or Partially-Conditioned Gaussian (PCG) [9], but they either lack the probabilistic interpretation of the correlation between the real and dual parts or still rely on local linearization. In [10]

978-0-9964527-7-9 ©2018 ISIF

and [11], a new distribution from the exponential family of probability density function is proposed to model uncertain dual quaternions and a UKF-like filtering scheme is developed. However, its assumed measurement model is restricted to be identity thus not suitable to be directly used for SLAM.

Second, states noise can be multi-modal, especially in real-world scenarios. This can be solved, e.g., by adapting the proposed distribution to mixture models as in [12] and [13]. However, they typically rely on an approximation in the Bayesian update step and are hard to be integrated into a probabilistic mapping block. Fig. 1 further gives an illustration of this issue. The depicted results are from a dual quaternion-based PF for overall 5 steps, where the magenta quivers and green curve indicate ground truth orientations and trajectory respectively. During each step, the dual quaternion particles are first translated by $\mathbf{t} = [15, 15]^T$ then rotated by $\theta = 30°$ respect to the last pose. Then they are propagated with uncertainty according to the distribution proposed in [10]. The system noise is zero-centered and a larger absolute diagonal entry in the parameter matrix $\mathbf{C}^w$ indicates a lower noise level. The simulated measurement noise has two independently distributed components, where the orientation part follows a zero-centered wrapped normal distribution [14] and the position measurement noise is Gaussian-distributed. Particles after update based on importance sampling are denoted by the red quivers. It is intuitive to see that the state particles tend to be multi-modal under higher system noise which can make the approximation to a uni-modal distribution risky during the update step.

Third, a SLAM system typically relies on multi-sensor fusion and possesses nonlinearity especially to the measurement model. This can be cleverly solved by using a progressive update approach [15] to the Bayesian update step as we proposed in [16], but it still relies on the sampling and re-approximation scheme and not suitable for multi-modal noise and mapping. Moreover, for our specific application scenarios where range and gyro sensors are employed, the typical probabilistic mapping approach is to use occupancy grid maps. The Monte Carlo localization approach can be further incorporated for handling the underlying nonlinearity as proposed in FastSLAM [17] where Rao–Blackwellization is used to reduce the high uncertainty space dimension. But conventional PF-based SLAM systems [17], [18] lack consideration of the nonlinear structure of the underlying manifold.

In this paper, we introduce a novel scheme of simultaneous localization and mapping for planar motions using low-cost range and gyro sensors. The SLAM system takes the idea of the grid-based FastSLAM [7] technique. Unlike the conventional PF where a Gaussian distribution is assumed to model the uncertain position and orientation angle, we use dual quaternions to represent $SE(2)$ states and further use a Bingham-like distribution to stochastically model them for particle generation and propagation. An occupancy grid map is hereby employed for the mapping part. In order to handle the potential high-dimensional uncertainty domain during Bayesian inference, we use Rao-Blackwellization for dimension reduction. Here, each dual quaternion is assigned with its own occupancy grid map and gets resampled during the update step given the likelihood of its observation. Our approach inherently considers the nonlinear structure of the $SE(2)$, allows multi-modal state noise and enables flexible sensor fusion for particle update, which shows promising potential for real-world SLAM scenarios.

In Sec. II, preliminaries such as pose representation using dual quaternions and the applied distribution from directional statistics are introduced. The core part is introduced in Sec. III including particle propagation and update as well as grid-based mapping. In Sec. IV, evaluation with both simulation and experiments are presented. The work is concluded and discussed finally in Sec. V.

II. Background

The theory of dual quaternions is essentially the combination of quaternions and dual theory, which was first introduced by Clifford [19]. For dual quaternion arithmetics, the readers can refer to [20] and [16]. Unit dual quaternions, which are dual quaternions of unit length, provide a convenient method for pose representation as well as manipulation in a similar manner as the unit quaternions do for orientation. In this section, we focus on introducing unit dual quaternions in the context of planar motions and further the Bingham-like distribution from the exponential family of density function for modeling uncertain planar dual quaternions.

A. Unit Dual Quaternions and Planar Motion

Without loss of generality, poses belonging to $SE(2)$ can be assumed to incorporate orientations around z-axis of angle θ and positions $\mathbf{t}$ in (x, y)-coordinates. Thus, the orientation quaternion can be represented by the following quaternion

$$\mathbf{x}_q = \cos\left(\frac{\theta}{2}\right) + \mathbf{k}\sin\left(\frac{\theta}{2}\right) . \tag{1}$$

Here, $\mathbf{k}$ denotes the unit vector along z-axis, such that $\mathbf{x}_q$ can be ensured to be of unit length via

$$\begin{aligned}
&\mathbf{x}_q \boxplus \mathbf{x}_q^* \\
&= \left(\cos\left(\frac{\theta}{2}\right) + \mathbf{k}\sin\left(\frac{\theta}{2}\right)\right) \boxplus \left(\cos\left(\frac{\theta}{2}\right) - \mathbf{k}\sin\left(\frac{\theta}{2}\right)\right) \\
&= \left(\cos\left(\frac{\theta}{2}\right)\right)^2 + \left(\sin\left(\frac{\theta}{2}\right)\right)^2 = 1 ,
\end{aligned}$$

with $\boxplus$ denoting the Hamilton product [21] and $\mathbf{x}_q^*$ the conjugate of $\mathbf{x}_q$. Given a unit quaternion representing the aforementioned rotation angle and axis, a vector $\mathbf{v} \in \mathbb{R}^2$ can be rotated to $\mathbf{v}'$ accordingly through $\mathbf{v}' = \mathbf{x}_q \boxplus \mathbf{v} \boxplus \mathbf{x}_q^*$. Moreover, unit quaternions representing planar orientations belong to the unit circle $\mathbb{S}^1$ in Euclidean space.

The dual quaternions are essentially two paired quaternions. In order to represent both positions and orientations, dual quaternions are defined as

$$\mathbf{x} = \mathbf{x}_q + \epsilon\, \mathbf{x}_p , \tag{2}$$

with $\mathbf{x}_q$ as in (1) representing the orientation part. Here ϵ denotes the dual unit with $\epsilon^2 = 0$ and the dual part, i.e., the translation quaternion, is defined as

$$\mathbf{x}_p = \frac{1}{2}\mathbf{t} \boxplus \mathbf{x}_q = \frac{1}{2}\mathbf{Q}_q \cdot \mathbf{t} , \tag{3}$$

which is half the product of position and orientation quaternion. Furthermore, there are overall three kinds of conjugate defined

for dual quaternions as introduced in Appendix A. The Hamilton product here can be also realized with the normal matrix-vector multiplication with

$$\mathbf{Q}_q = \begin{pmatrix} x_{q,1} & x_{q,2} \\ -x_{q,2} & x_{q,1} \end{pmatrix} \in SO(2)\,, \tag{4}$$

which is a two-dimensional rotation matrix. A proof can be found in Appendix B. With real and dual part defined as in (1) and (3) respectively, the dual quaternions in (2) are inherently guaranteed to be of unit length. A vector $\mathbf{v} \in \mathbb{R}^2$ can also be transformed to $\mathbf{v}'$ by getting first rotated by $\mathbf{x}_q$ then translated by $\mathbf{t}$ via

$$\mathbf{v}' = \mathbf{x} \boxplus \mathbf{v} \boxplus \mathbf{x}^\circ\,, \tag{5}$$

with $\mathbf{x}^\circ = \mathrm{diag}(1,-1,1,1) \cdot \mathbf{x}$ denoting the full conjugate of the dual quaternion $\mathbf{x}$. The unit dual quaternions give a convenient method for performing planar transformation in a similar manner as unit quaternions do for planar rotation. Corresponding proofs are presented in Appendix C and D respectively. The manifold of unit dual quaternions representing planar motions is thus the Cartesian product of the unit circle and the two-dimensional Euclidean space and it is embedded in the four-dimensional Euclidean space, namely

$$\mathbf{x} = \begin{bmatrix} \mathbf{x}_q \\ \mathbf{x}_p \end{bmatrix} \in \mathbb{S}^1 \times \mathbb{R}^2 \subset \mathbb{R}^4\,, \tag{6}$$

Furthermore, two antipodal unit dual quaternions, namely $\mathbf{x}$ and $-\mathbf{x}$ denote the same planar rigid body motion.

B. Stochastic Modeling of Uncertain Dual Quaternions

In order to generate unit dual quaternion particles for our SLAM system, a distribution proposed in [10] and [22] is employed. It belongs to the exponential family, inherently incorporates the underlying nonlinear structure of $SE(2)$ states and gives further consideration of correlation between orientation and position. The proposed distribution is defined as

$$f(\mathbf{x}) = \frac{1}{N(\mathbf{C})} \exp(\mathbf{x}^T \mathbf{C} \mathbf{x})\,, \tag{7}$$

with $\mathbf{x}$ denoting dual quaternions of $SE(2)$ states in (5). The parameter matrix $\mathbf{C}$ is defined as

$$\mathbf{C} = \begin{pmatrix} \mathbf{C}_1 & \mathbf{C}_2^T \\ \mathbf{C}_2 & \mathbf{C}_3 \end{pmatrix}\,, \tag{8}$$

with $\mathbf{C}_i \in \mathbb{R}^{2\times 2}$, symmetric $\mathbf{C}_1$, arbitrary $\mathbf{C}_2$ and symmetric negative definite $\mathbf{C}_3$. It also determines the normalization constant $N(\mathbf{C})$ [10]. The distribution can be further decomposed as

$$\begin{aligned} f(\mathbf{x}) &= f_{\mathbf{x}_q}(\mathbf{x}_q) f_{\mathbf{x}_p|\mathbf{x}_q}(\mathbf{x}_p|\mathbf{x}_q) \\ &= \frac{1}{N(\mathbf{C})} \exp(\mathbf{x}_q^T \mathbf{T}_1 \mathbf{x}_q + (\mathbf{x}_p - \mathbf{T}_2\mathbf{x}_q)^T \mathbf{C}_3 (\mathbf{x}_p - \mathbf{T}_2 \mathbf{x}_q))\,, \end{aligned}$$

with $\mathbf{T}_1 = \mathbf{C}_1 - \mathbf{C}_2^T \mathbf{C}_3^{-1} \mathbf{C}_2$ and $\mathbf{T}_2 = \mathbf{C}_3^{-1} \mathbf{C}_2$. Thus, it can be viewed as the product of a Bingham distribution [23] modeling the orientation part and a Gaussian distribution modeling the translation part conditioned on each individual orientation, i.e.,

$$\mathbf{x}_q \sim \mathcal{B}(\mathbf{T}_1),\ \mathbf{x}_p|\mathbf{x}_q \sim \mathcal{N}(\mathbf{T}_2\mathbf{x}_q, -0.5\mathbf{C}_3^{-1})\,. \tag{9}$$

The distribution is antipodally symmetric since $f(\mathbf{x}) = f(-\mathbf{x})$. Some detailed probabilistic interpretation of the applied distribution can also be found in [16].

III. Grid-based SLAM Using Dual Quaternion Particle Filter

In this paper, we specify our application scenario to be planar SLAM using on-board range and gyro sensors with robot pose represented by unit dual quaternions. From a probabilistic viewpoint, a full SLAM problem is formalized as estimating the posterior of both the poses $\mathbf{x}$ and map $\mathcal{M}$ of all time steps, i.e.,

$$p(\mathbf{x}_{0:k}, \mathcal{M} | \mathbf{z}_{1:k}, \mathbf{u}_{1:k})\,. \tag{10}$$

Here $\mathbf{x}_{0:k} \in \mathbb{S}^1 \times \mathbb{R}^2$ denote overall robot pose chain, $\mathbf{z}_{1:k}$ and $\mathbf{u}_{1:k}$ are the measurements and system input up to the current time step k respectively.

We propose a recursive estimation scheme for pose tracking and use grid-based occupancy maps for mapping. In order to handle the potential case of multi-modal noise, we use an approach based on particle filtering with dual quaternion states. The particles are generated according to the distribution in (7) and get propagated through

$$\mathbf{x}_{k+1} = a(\mathbf{x}_k, \mathbf{u}_k) \boxplus \mathbf{w}_k\,, \tag{11}$$

with $a(\cdot,\cdot)$ denoting the system equation and $\mathbf{w}_k \in \mathbb{S}^1 \times \mathbb{R}^2$ the dynamics noise. Due to the advantages discussed in II-B, the system noise is assumed to follow also the aforementioned distribution in (7) . Each particle gives a hypothesis of the robot pose and has its own estimated map based on its observation given the measurement model

$$\mathbf{z}_k = h(\mathbf{x}_k) \otimes \mathbf{v}_k\,, \tag{12}$$

with function $h(\cdot)$ mapping the dual quaternion state to the measurement domain. Here, the measurement noise $\mathbf{v}_k$ can be either additive or non-additive (denoted by $\otimes$, which is invertible) and it can be of arbitrary measurement domain. The dual quaternion particles are then resampled according to its observation likelihood and the global map also gets updated correspondingly. A grid-based mapping approach is used here by which the map is discretized into

$$\mathcal{M} = \{\mathbf{m}_i\}_{i=1:m}\,, \tag{13}$$

with $\mathbf{m}_i$ denoting the map grid cell indexed by i.

In this section, we focus on presenting the central blocks of our proposed SLAM scheme including the tracking method based on particle filtering using dual quaternions as well as the mapping technique based on occupancy grid maps.

A. Rao-Blackwellization for Grid-based SLAM

Since our approach is PF-based, directly sampling in the posterior domain formalized in (10) typically suffers from the curse of dimensionality. We thus decompose the full SLAM posterior based on Rao-Blackwellization [7] into, i.e.,

$$\begin{aligned} &p(\mathbf{x}_{0:k}, \mathcal{M} | \mathbf{z}_{1:k}, \mathbf{u}_{1:k}) = \\ &\qquad p(\mathbf{x}_{0:k} | \mathbf{z}_{1:k}, \mathbf{u}_{1:k}) \cdot p(\mathcal{M} | \mathbf{x}_{1:k}, \mathbf{z}_{1:k}, \mathbf{u}_{1:k})\,, \end{aligned} \tag{14}$$

where the first part denotes the trajectory posterior and the second part denotes the map posterior. However, direct

estimation of the map posterior for each single particle can also be intractable especially in the case of large-scale mapping, as the posterior is actually the joint probability of all the grid cells $\mathbf{m}_i$. A typical solution used in grid-based SLAM is to assume each of the cell occupancy to be independently distributed such that the map posterior can be approximated as the product of all the marginals

$$p(\mathcal{M}|\mathbf{z}_{1:k}, \mathbf{u}_{1:k}) = \prod_{i=1}^{m} p(\mathbf{m}_i|\mathbf{z}_{1:k}, \mathbf{u}_{1:k}) \,, \tag{15}$$

with $p(\mathbf{m}_i|\mathbf{z}_{1:k}, \mathbf{u}_{1:k})$ denoting the probability that cell $\mathbf{m}_i$ is occupied. With the assumption in (14) and (15), a tractable grid-based SLAM formalization can be derived as

$$\begin{aligned} &p(\mathbf{x}_{0:k}, \mathcal{M}|\mathbf{z}_{1:k}, \mathbf{u}_{1:k}) = \\ &\qquad p(\mathbf{x}_{0:k}|\mathbf{z}_{1:k}, \mathbf{u}_{1:k}) \cdot \prod_{i=1}^{m} p(\mathbf{m}_i|\mathbf{x}_{1:k}, \mathbf{z}_{1:k}) \,. \end{aligned} \tag{16}$$

B. Occupancy Grid Mapping

Mapping with low-cost sensors, e.g., ultrasonic sensors, can suffer from the common issue of high measurement noise level as well as very sparse measurement resolution. One of the most popular mapping approaches for range sensor perception is to use an occupancy grid map, where the map gets discretized into grid cells assigned to the occupancy probabilities, namely the probability of a cell being occupied or obstacle-free. For better numerical stability, the posterior occupancy probability of the i_{th} cell in (15) is typically represented in its *log odds* form, namely

$$l_{k,i} = \log\left(\frac{p(\mathbf{m}_i|\mathbf{x}_{1:k}, \mathbf{z}_{1:k})}{1 - p(\mathbf{m}_i|\mathbf{x}_{1:k}, \mathbf{z}_{1:k})}\right) .$$

Since the occupancy probability of each cell is typically initialized to be 0.5, we have the log odds

$$l_{0,i} = \log(0.5/(1 - 0.5)) = 0 \,.$$

At each recursive estimation step, the sensor takes a new measurement and the occupancy map should also be updated, for which the *inverse sensor model* is typically applied, i.e.,

$$g(\mathbf{m}_i, \mathbf{x}_k, \mathbf{z}_k) = \log\left(\frac{p(\mathbf{m}_i|\mathbf{x}_k, \mathbf{z}_k)}{1 - p(\mathbf{m}_i|\mathbf{x}_k, \mathbf{z}_k)}\right) . \tag{17}$$

Compared to the forward sensor model $p(\mathbf{z}_k|\mathbf{x}_k, \mathbf{m}_i)$, the inverse sensor model gives occupancy probability hypothesis based on the measurement. Regarding the ultrasonic sensors, for instance, the inverse sensor model represents the functional principle of a measurement by means of creating a cone with a filling that has the probability of being free and endpoints with a probability of being occupied [7, Table 9.2]. The log odds occupancy of cell i can thus be updated using the binary Bayes filter [7, Table 4.2] according to

$$l_{k,i} = l_{k-1,i} + g(\mathbf{m}_i, \mathbf{x}_k, \mathbf{z}_k) - l_{0,i} \,, \tag{18}$$

where $l_{k,i}$ and $l_{k-1,i}$ denote the log odds occupancy of the current and the last time step respectively. The posterior occupancy probability of cell $\mathbf{m}_i$ after updating with the current measurement can then be computed as

$$p(\mathbf{m}_i|\mathbf{z}_{1:k}, \mathbf{x}_{1:k}) = 1 - \frac{1}{1 + \exp(l_{k,i})} \,.$$

A detailed algorithm for updating the occupancy grid maps of all dual quaternion particles $\{\mathbf{x}_{k,j}\}_{j=1:n}$ given the current measurement $\mathbf{z}_k$ is introduced in Alg. 1. The function in line 4 updates each cell of the old map $\mathcal{M}_{k-1,j}$ with the newly calculated occupancy log odds.

Algorithm 1 Occupancy Grid Map Update

procedure updateMap $(\mathbf{z}_k, \{(\mathbf{x}_{k,j}, \mathcal{M}_{k-1,j})\}_{j=1:n})$
1: **for** $j = 1$ to n **do**
2: **for** $i = 1$ to m **do**
3: $l_{k,i} \leftarrow l_{k-1,i} + g(\mathbf{m}_{k-1,j,i}, \mathbf{x}_{k,j}, \mathbf{z}_k) - l_{0,i}$;
4: $\mathcal{M}_{k,j} \leftarrow$ updateCellOccupancy $(\mathcal{M}_{k-1,j}, l_{k,i})$;
5: **end for**
6: **end for**
7: **return** $\{\mathcal{M}_{k,j}\}_{j=1:n}$
end procedure

C. Particle Generation

Dual quaternion particles are generated by random sampling on the manifold $\mathbb{S}^1 \times \mathbb{R}^2$ in a manner according to the conditional probability introduced in (9). First, we randomly sample the rotation quaternions from the Bingham part [24]. Second, conditioned on each orientation quaternion particle we sample from the Gaussian for the translation quaternion part. In the end we give the dual quaternion particles by concatenating the two sets. The detailed sampling scheme is introduced in Alg. 2.

Algorithm 2 Particle Generation

procedure sampleRandom $(\mathbf{C}, n)$
1: $\mathbf{T}_1 \leftarrow \mathbf{C}_1 - \mathbf{C}_2^T \mathbf{C}_3^{-1} \mathbf{C}_2$;
2: $\mathbf{T}_2 \leftarrow -\mathbf{C}_3^{-1} \mathbf{C}_2$;
3: $\{\mathbf{x}_{q,j}\}_{j=1\cdots,n} \leftarrow$sampleRandomBingham $(\mathbf{T}_1)$;
4: $\{\mathbf{x}_{p,j}\}_{j=1\cdots,n} \leftarrow$sampleRandomGaussian $(\mathbf{0}, -0.5\mathbf{C}_3^{-1})$;
5: **for** $j = 1$ to n **do**
6: $\mathbf{x}_{p,j} \leftarrow \mathbf{T}_2 \mathbf{x}_{q,j} + \mathbf{x}_{p,j}$;
7: $\mathbf{x}_j \leftarrow [\mathbf{x}_{q,j}^T, \mathbf{x}_{p,j}^T]^T$;
8: **end for**
9: **return** $\{\mathbf{x}_j\}_{j=1:n}$
end procedure

D. Particle Prediction

For each recursive step, the dual quaternion particles estimated from last step $\{\mathbf{x}_{k-1,j}^e\}_{j=1:n}$ are propagated through the system equation $a(\cdot, \cdot)$ and further propagated with uncertain noise terms that are also randomly sampled from the system noise distribution characterized by $\mathbf{C}^w$. The detailed approach is introduced in Alg. 3.

Algorithm 3 Particle Prediction

procedure predictParticles $(\mathbf{u}_k, \{\mathbf{x}^e_{k-1,j}\}_{j=1:n})$
1: $\{\mathbf{x}_{w,j}\}_{j=1:n} \leftarrow$sampleRandom $(\mathbf{C}^w)$;
2: **for** $j = 1$ to n **do**
3: $\quad \mathbf{x}^p_{k,j} \leftarrow a(\mathbf{x}^e_{k-1,j}, \mathbf{u}_k) \boxplus \mathbf{x}_{w,j}$;
4: **end for**
5: **return** $\{\mathbf{x}^p_{k,j}\}_{j=1:n}$
end procedure

E. Particle Update

In general, the update step follows the same idea of the Rao-Blackwellized particle filter based on the occupancy grid map. Here, dual quaternion particles are resampled according to their likelihoods. More specifically, given the measurement model (for both additive and non-additive noise) in (12), the likelihood for a dual quaternion particle given the current measurement $\mathbf{z}_k$ can be computed using Bayes' theorem as follows

$$\begin{aligned} & f(\mathbf{z}_k|\mathbf{x}_{k,j}) \\ &= \int_{\mathcal{Z}} f(\mathbf{z}_k, \mathbf{v}_k|\mathbf{x}_{k,j}) d\mathbf{v}_{k,j} \\ &= \int_{\mathcal{Z}} f(\mathbf{z}_k|\mathbf{v}_{k,j}, \mathbf{x}_{k,j}) f(\mathbf{v}_{k,j}) d\mathbf{v}_{k,j} \\ &= \int_{\mathcal{Z}} \delta(\mathbf{v}_{k,j} - (h_{\mathcal{M}_j}(\mathbf{x}_{k,j}))^{-1} \otimes \mathbf{z}_k) f(\mathbf{v}_{k,j}) d\mathbf{v}_{k,j} \\ &= f_{\mathbf{v}}((h_{\mathcal{M}_j}(\mathbf{x}_{k,j}))^{-1} \otimes \mathbf{z}_k)\,, \end{aligned} \tag{19}$$

with $\mathcal{Z}$ denoting the measurement domain and $f_{\mathbf{v}}$ the measurement noise distribution. As mentioned in (12), the function $h_{\mathcal{M}_j}(\cdot) : \mathbb{S}^1 \times \mathbb{R}^2 \mapsto \mathcal{Z}$ gives a measurement hypothesis for each dual quaternion particle $\mathbf{x}_j$.

For our application scenario where range sensors are employed, this function is implemented based on the *likelihood field model* [7, Chapter 6.4], in which the range measurement hypothesis is given by calculating its Euclidean distance to the nearest occupied cell of the estimated grid map assigned to the particle $\mathbf{x}_{k,j}$. If no obstacle cell is found by $\mathbf{x}_j$, its likelihood is directly assigned to a value indicating the uniform distribution, i.e., $f(\mathbf{z}_k|\mathbf{x}_{k,j}) = 1/d_{\max}$, with $d_{\max}$ denoting the maximum range. The dual quaternion particles can then be resampled based on selective sampling given their likelihoods, in which we first calculate the normalized Effective Sample Size (ESS) [25] defined as

$$\frac{1}{ESS} = n \cdot \sum_{j=1}^{n} w_j\,,$$

with n denoting particle size. And the importance sampling is only performed when the ESS is less than a given threshold, e.g., 0.5. The scheme for updating particles can be found in Alg. 4.

F. SLAM Using Dual Quaternion Particles

The full scheme of the proposed SLAM approach comprises the aforementioned mapping and particle filtering components. For each recursive step, as shown in Alg. 5, we first propagate the dual quaternion particles according to the system equation and the assumed noise distribution, then update the occupancy grid map and finally update the particles based on selective resampling according to the likelihood field. In order to visualize a globally consistent map after each recursive step, each grid cell is given a log odds occupancy by the particle with the largest weight.

Algorithm 4 Particle Update

procedure updateParticles $(\{(\mathbf{x}^p_{k,j}, \mathcal{M}^e_{k,j})\}_{j=1:n}, \mathbf{z}_k)$
1: $\{(\mathbf{x}^e_{k,j}, w_{k,j})\}_{j=1:n} \leftarrow \emptyset$;
2: **for** $j = 1$ to n **do**
3: $\quad w_{k,j} \leftarrow f_{\mathbf{v}}((h_{\mathcal{M}^e_{k,j}}(\mathbf{x}^p_{k,j}))^{-1} \otimes \mathbf{z}_k)$;
4: **end for**
5: $\{\mathbf{x}^e_{k,j}\}_{j=1:n} \leftarrow$selectiveResample $(\{\mathbf{x}^p_{k,j}\}_{j=1:n}, w_{k,j})$;
6: **return** $\{(\mathbf{x}^e_{k,j}, w_{k,j})\}_{j=1:n}$
end procedure

Algorithm 5 SLAM with Dual Quaternion Particles

procedure DQPFSLAM $(\{(\mathbf{x}^e_{k-1,j}, \mathcal{M}^e_{k-1,j})\}_{j=1:n}, \mathbf{u}_k, \mathbf{z}_k)$
1: $\{\mathbf{x}^p_{k,j}\}_{j=1:n} \leftarrow$ predictParticles $(\mathbf{u}_k, \{\mathbf{x}^e_{k-1,j}\}_{j=1:n})$;
2: $\{\mathcal{M}^e_{k,j}\}_{j=1:n} \leftarrow$ updateMap $(\mathbf{z}_k, \{(\mathbf{x}^p_{k,j}, \mathcal{M}^e_{k-1,j})\}_{j=1:n})$;
3: $\{(\mathbf{x}^e_{k,j}, w_{k,j})\}_{j=1:n} \leftarrow$ updateParticles (
4: $\qquad\qquad \{(\mathbf{x}^p_{k,j}, \mathcal{M}^e_{k,j})\}_{j=1:n}, \mathbf{z}_k)$;
5: **return** $\{(\mathbf{x}^e_{k,j}, \mathcal{M}^e_{k,j})\}_{j=1:n}$
end procedure

IV. Evaluation

In this section, the proposed SLAM approach is evaluated with a miniature walking robot (shown in Fig. 2) performing planar rigid body motions in a static and unknown environment. The robot aims to estimate its own poses and simultaneously map the unknown surroundings using low-cost on-board sensors, which are four ultrasonic sensors and an IMU. The evaluation is performed in both simulated and real-world experiment scenarios.

For each step of movement, the robot is given a dual quaternion input $\mathbf{u}_k \in \mathbb{S}^1 \times \mathbb{R}^2$ following a dynamics model

$$\mathbf{x}_{k+1} = \mathbf{x}_k \boxplus \mathbf{u}_k \boxplus \mathbf{w}_k\,, \tag{20}$$

with the noise term $\mathbf{w}_k \in \mathbb{S}^1 \times \mathbb{R}^2$ following the distribution introduced in (7) characterized by a parameter matrix $\mathbf{C}^w = \mathrm{diag}(-1, -100, -100, -100)$ indicating zero-centered noise. The measurement domain $\mathcal{Z} = \mathbb{S}^1 \times \mathbb{R}^4$, which comprises the orientation measurement $\mathbf{q}_k \in \mathbb{S}^1$ from the IMU and four range measurements $\mathbf{d}_k = [d^1_k, d^2_k, d^3_k, d^4_k]^T \in \mathbb{R}^4$ from the ultrasonic sensors. The IMU measurement is assumed to have a non-additive and zero-centered noise that is Bingham-distributed characterized by $\mathbf{C}^{\text{ort}} = \mathrm{diag}(0, -50)$. The noise of each range measurement is assumed to be additive and Gaussian-distributed as $\mathbf{v}_d \sim \mathcal{N}(0, 2)$. We further assume that all of the measurement noises are independently distributed, thus the likelihood of particle $\mathbf{x}_{k,j}$ during the update step can be calculated by simply taking the product of each, i.e.,

$$\begin{aligned} & f(\mathbf{z}_k|\mathbf{x}_{k,j}) \\ &= f_{\mathbf{v}_q}(\mathbf{x}^{-1}_{k,q} \boxplus \mathbf{q}_k) \prod_{r=1}^{4} f_{\mathbf{v}_d}(d^r_k - s^r_{\mathcal{M}_{k,j}}(\mathbf{x}_{k,j}))\,, \end{aligned} \tag{21}$$

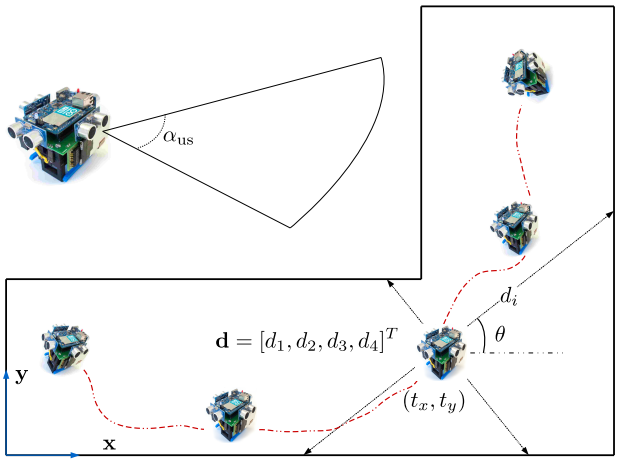

Figure 2: Sketches of a walking robot equipped with four ultrasonic sensors and an IMU performing planar rigid body motions in static obstacles.

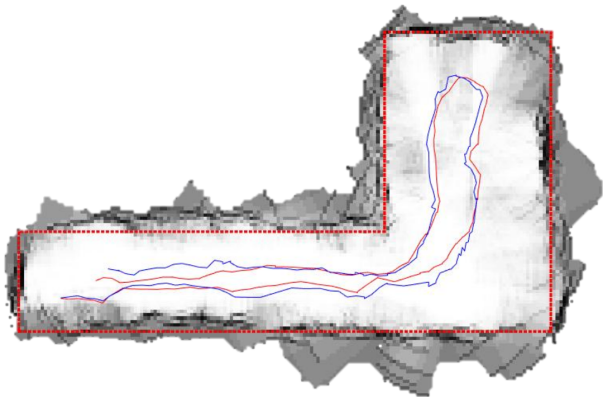

Figure 3: Estimated map and trajectory using our proposed SLAM approach. The red and blue curve denote the ground truth and estimated trajectory respectively and the mapping ground truth is shown with red dot curve.

where the function $s^r_{\mathcal{M}_{k,j}}(\cdot)$ gives the expected distance measurement based on the occupancy grid map assigned to the particle. In the case of unknown areas, the likelihood for single range measurement is assumed to be uniformly distributed, i.e., $f_{\mathbf{v}_d} = 1/d_{\text{max}}$, with maximum detection range $d_{\text{max}} = 50\,\text{cm}$, as discussed in III-E.

The evaluations are performed as follows. First, simulations are carried out with an emphasis of showing the possibility of employing our proposed SLAM approach for simultaneous tracking and mapping. Second, a real-world scenario is designed in which the previously mentioned robot navigates in an unknown environment and the tracking accuracy is evaluated for both orientation and position based on multiple Monte Carlo runs. In both simulation and experiment, the ultrasonic sensor has a beam angle $\alpha_{\text{us}} = 15^\circ$ and an effective detection range of $2\,\text{cm} \sim 65\,\text{cm}$. And the robot is able to move for about $1.6\,\text{cm}$ in each direction and rotate for 16° per step. The implementation of our proposed SLAM approach is based on [26].

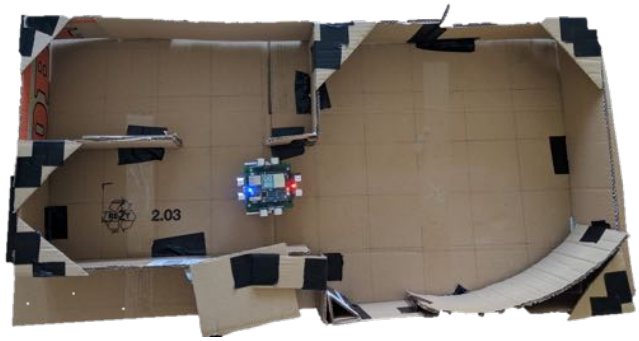

Figure 4: Robot navigating in the experimental setup. Using our proposed SLAM approach, the robot aims to estimate itself for both orientation and position in an unknown environment with surrounding cardboard obstacles.

A. *Simulation Scenario*

During the simulation run, the robot is ordered to move stepwise in an environment of similar shape as in Fig. 2 without predefined map information. The map has an approximated area of $7800\,\text{cm}^2$. Fig. 3 shows the tracking result as well as the result of grid-based mapping. The estimated occupancy map is visualized by directly taking the log odds of each cell as a grayscale pixel, with a larger intensity indicating a higher probability of being occupied by obstacles, e.g., the black pixels. Despite of the high-level noise and sparse perception of the ultrasonic sensors, our approach is still able to give a reasonable reconstruction of the map and a good estimation of the trajectory. We get the result from a single simulation run with 200 dual quaternion particles.

B. *Experiment Scenario*

For the first time, filtering approaches based on the proposed distribution in [10] are evaluated in a real-world scenario. Here we set up an environment with static obstacles shown in Fig. 4, which is unknown for the robot. During the controlled and stepwise movements in the map, the robot aims to localize itself by using the on-board four ultrasonic sensors and IMU. For this specific test case, both of the system and measurement noise level can be very high, partially due to the fact that, e.g., the robot is likely to slip, the low-cost ultrasonic sensors can give unreliable measurements, and the potential multiple reflection among the walls as well as the drift issue of IMU cannot be ignored. The ground truth of robot's pose is measured by using a ceiling camera from above. Due to the aforementioned issues, only tracking accuracy is evaluated.

We compare the tracking accuracy of our proposed SLAM system based on dual quaternion particles with the SLAM systems based on the ordinary particle filter as well as the progressive dual quaternion filter [16]. In order to have the same noise level of system dynamics between the ordinary PF and the dual quaternion-based filters, we approximate the Gaussian distribution of the ordinary PF from dual quaternion samples randomly drawn from the distribution in (20). And we apply the same Bingham-distributed orientation noise for all the filters. The evaluation is performed based on 100 Monte Carlo runs of one single recorded dataset and the result is

depicted in Fig. 5. Because all of the filtering approaches use roughly the same orientation distribution for system noise, the orientation RMS errors of the three approaches are on the same level. However, our proposed dual quaternion particle filter outperforms the others for position estimation. This is mainly because our proposed approach gives better consideration of the nonlinearity underlying the structure of $SE(2)$ compared to the ordinary PF and is able to handle the multi-modal noise compared to the progressive dual quaternion filter where the noise is assumed to be uni-modal.

V. Conclusion and Outlook

In this paper, we presented a novel SLAM approach using range and gyro sensors based on a dual quaternion particle filter. This approach incorporates a better understanding of the nonlinear structures of $SE(2)$ by using unit dual quaternions for pose representation and the proposed distribution introduced in II-B to propagate system uncertainty. Moreover, the particle-based filtering approach is able to handle multi-modal noise distribution, which theoretically outperforms the approaches based on uni-modal noise distribution, e.g., [22] and [16]. The proposed filtering approach using dual quaternion particles is further integrated with grid-based mapping methods into a full SLAM scheme based on Rao-Blackwellization. The proposed SLAM system is able to give reasonable mapping results and outperforms the typical uni-modal-assumed filters as well as ordinary PF for pose estimation in real-world scenarios.

There are still a few corresponding extensions that can be made in the future. For example, the proposed filter is only for performing tracking on a plane. It would be appealing to extend this filtering approach to general spatial movements, namely the group $SE(3)$. Second, the aforementioned SLAM system is designed for range sensor-based perception scenarios where the occupancy grid map is employed. It should be possible to further integrate this dual quaternion particle-based approach into some more generic SLAM scenarios, e.g., some visual-based perception or SLAM systems. Third, efficiency issue is not discussed in this paper. However, it should be investigated later for its employment in practical applications.

Appendix

A. Dual Quaternion Conjugates

For an arbitrary dual quaternion defined as in (2), whose vector form $\mathbf{x} \in \mathbb{R}^8$, it has overall three kinds of conjugates as follows. First, the *dual conjugate* takes the conjugate of the dual unit ϵ and can be written as

$$\mathbf{x}^{\bullet} = \mathrm{diag}(1,1,1,1,-1,-1,-1,-1) \cdot \mathbf{x}\,.$$

Second, the *classical conjugate* only conjugates each individual quaternion, namely

$$\mathbf{x}^{*} = \mathrm{diag}(1,-1,-1,-1,1,-1,-1,-1) \cdot \mathbf{x}\,.$$

Third, the *full conjugate* combines the former two conjugations as

$$\mathbf{x}^{\circ} = (\mathbf{x}^{\bullet})^{*} = \mathrm{diag}(1,-1,-1,-1,-1,1,1,1) \cdot \mathbf{x}\,.$$

B. Proof 1

Since $\mathbf{x}_q \in \mathbb{S}^1$, it can be proven that

$$\mathbf{Q}_q \mathbf{Q}_q^T = \begin{pmatrix} x_{q,1} & x_{q,2} \\ -x_{q,2} & x_{q,1} \end{pmatrix} \begin{pmatrix} x_{q,1} & -x_{q,2} \\ x_{q,2} & x_{q,1} \end{pmatrix} = \mathbf{I}_{2\times 2}\,.$$

Similarly we also have $\mathbf{Q}_q^T \mathbf{Q}_q = \mathbf{I}_{2\times 2}$. Moreover, we have

$$\det(\mathbf{Q}_q) = ||\mathbf{x}_q|| = 1\,,$$

thus it belongs to the two-dimensional rotation matrix group, i.e., $\mathbf{Q}_q \in SO(2)$.

C. Proof 2

With the real and dual part of a dual quaternion defined as (1) and (3), the norm of it can be computed as follows

$$\begin{aligned}
\mathbf{x} \boxplus \mathbf{x}^{*} &= (\mathbf{x}_q + \epsilon\, \mathbf{x}_p) \boxplus (\mathbf{x}_q^{*} + \epsilon\, \mathbf{x}_p^{*}) \\
&= \mathbf{x}_q \boxplus \mathbf{x}_q^{*} + \epsilon\, (\mathbf{x}_q \boxplus \mathbf{x}_p^{*} + \mathbf{x}_p \boxplus \mathbf{x}_q^{*}) \\
&= \mathbf{x}_q \boxplus \mathbf{x}_q^{*} + \frac{\epsilon}{2} (\mathbf{x}_q \boxplus \mathbf{x}_q^{*} \boxplus \mathbf{t}^{*} + \mathbf{t} \boxplus \mathbf{x}_q \boxplus \mathbf{x}_q^{*}) \\
&= \mathbf{x}_q \boxplus \mathbf{x}_q^{*} + \frac{\epsilon}{2} (\mathbf{t}^{*} + \mathbf{t}) \\
&= \mathbf{x}_q \boxplus \mathbf{x}_q^{*} = 1\,.
\end{aligned}$$

Here $\epsilon^2 = 0$ and the conjugate of vector $\mathbf{t}$ in quaternion form is simply its opposite. Moreover, $\mathbf{x}^{*}$ denotes the classical conjugate of the dual quaternion $\mathbf{x}$ where each of its composing quaternion is conjugated.

D. Proof 3

Given a unit dual quaternion defined in (6) for planar motions, a vector $\mathbf{v} \in \mathbb{R}^2$ can get transformed according to

$$\begin{aligned}
\mathbf{v}' &= \mathbf{x} \boxplus \mathbf{v} \boxplus \mathbf{x}^{\circ} \\
&= (\mathbf{x}_q + \frac{\epsilon}{2} \mathbf{t} \boxplus \mathbf{x}_q) \boxplus (1 + \epsilon\, \mathbf{v}) \boxplus (\mathbf{x}_q + \frac{\epsilon}{2} \mathbf{t} \otimes \mathbf{x}_q)^{\circ} \\
&= (\mathbf{x}_q + \epsilon\, \mathbf{x}_q \boxplus \mathbf{v} + \frac{\epsilon}{2} \mathbf{t} \boxplus \mathbf{x}_q) \boxplus (\mathbf{x}_q^{*} - \frac{\epsilon}{2} \boxplus \mathbf{x}_q^{*} \otimes \mathbf{t}^{*}) \\
&= \mathbf{x}_q \boxplus \mathbf{x}_q^{*} + \epsilon\, \mathbf{x}_q \boxplus \mathbf{v} \otimes \mathbf{x}_q^{*} + \\
&\qquad \frac{\epsilon}{2} (\mathbf{t} \boxplus \mathbf{x}_q \otimes \mathbf{x}_q^{*} - \mathbf{x}_q \boxplus \mathbf{x}_q^{*} \boxplus \mathbf{t}^{*}) \\
&= 1 + \epsilon\, (\mathbf{x}_q \boxplus \mathbf{v} \boxplus \mathbf{x}_q^{*} + \mathbf{t})\,,
\end{aligned}$$

where $\mathbf{v}$ first gets rotated by rotation quaternion $\mathbf{x}_q$ then translated by $\mathbf{t}$.

Acknowledgment

This work is supported by the German Research Foundation (DFG) under grant HA 3789/16-1 "*Recursive Estimation of Rigid Body Motions*".

References

[1] K. Granström, "Extended target tracking using PHD filters," Ph.D. dissertation, Linköping University Electronic Press, 2012.

[2] J. Zhu, "Image gradient-based joint direct visual odometry for stereo camera," in *Int. Jt. Conf. Artif. Intell*, 2017, pp. 4558–4564.

[3] J. Engel, J. Stückler, and D. Cremers, "Large-scale direct SLAM with stereo cameras," in *2015 IEEE/RSJ International Conference on Intelligent Robots and Systems (IROS)*. IEEE, 2015, pp. 1935–1942.

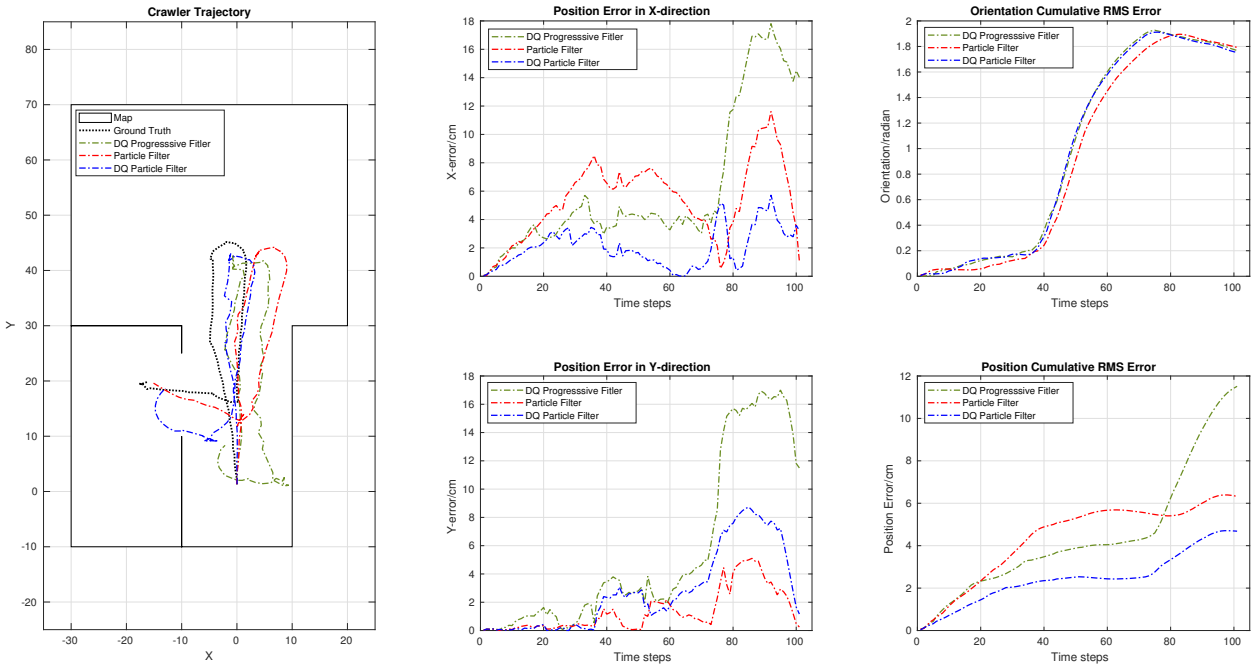

Figure 5: Evaluation result for robot tracking in the real-world experiment set up in Fig.4. The picture on the left shows the digitalized cardboard map. In the map, we plot the estimated trajectory using our proposed filtering approach (blue), the ordinary particle filter (red) and the progressive filtering approach [16] (green). We plot the cumulative RMS error to show the tracking accuracy and the per-step error on x and y to show how the error evolves. The results are based on 100 Monte Carlo runs based on the same recorded data using 200 dual quaternion particles.

[4] F. Dellaert, D. Fox, W. Burgard, and S. Thrun, "Monte carlo localization for mobile robots," in *Proceedings 1999 IEEE International Conference on Robotics and Automation*, vol. 2. IEEE, 1999, pp. 1322–1328.

[5] H. Temeltas and D. Kayak, "SLAM for robot navigation," *IEEE Aerospace and Electronic Systems Magazine*, vol. 23, no. 12, pp. 16–19, 2008.

[6] S. J. Julier and J. K. Uhlmann, "Unscented filtering and nonlinear estimation," *Proceedings of the IEEE*, vol. 92, no. 3, pp. 401–422, 2004.

[7] S. Thrun, W. Burgard, and D. Fox, *Probabilistic Robotics*. MIT press, 2005.

[8] J. Goddard, "Pose and motion estimation from vision using dual quaternion-based extended Kalman filtering. University of Tennessee, Knoxville," Ph.D. dissertation, 1997.

[9] J. E. Darling and K. J. DeMars, "Uncertainty Propagation of correlated quaternion and Euclidean states using partially-conditioned Gaussian mixtures," in *19th International Conference on Information Fusion (FUSION)*, July 2016, pp. 1805–1812.

[10] I. Gilitschenski, G. Kurz, S. J. Julier, and U. D. Hanebeck, "A new probability distribution for simultaneous representation of uncertain position and orientation," in *17th International Conference on Information Fusion (FUSION)*. IEEE, 2014.

[11] ——, "Unscented orientation estimation based on the Bingham distribution," *IEEE Transactions on Automatic Control*, vol. 61, no. 1, pp. 172–177, 2016.

[12] M. Lang and W. Feiten, "MPG-fast forward reasoning on 6 dof pose uncertainty," in *ROBOTIK 2012; 7th German Conference on Robotics*. VDE, 2012, pp. 1–6.

[13] W. Feiten, M. Lang, and S. Hirche, "Rigid motion estimation using mixtures of projected gaussians," in *16th International Conference on Information Fusion (FUSION)*. IEEE, 2013, pp. 1465–1472.

[14] K. V. Mardia and P. E. Jupp, *Directional statistics*. John Wiley & Sons, 2009, vol. 494.

[15] J. Steinbring and U. D. Hanebeck, "Progressive Gaussian filtering using explicit likelihoods," in *17th International Conference on Information Fusion (FUSION)*, July 2014.

[16] K. Li, G. Kurz, L. Bernreiter, and U. D. Hanebeck, "Nonlinear progressive filtering for $SE(2)$ Estimation," in *21st International Conference on Information Fusion (FUSION)*. IEEE, 2018.

[17] M. Montemerlo, S. Thrun, D. Koller, B. Wegbreit *et al.*, "FastSLAM: A factored solution to the simultaneous localization and mapping problem," *Aaai/iaai*, vol. 593598, 2002.

[18] M. Montemerlo and S. Thrun, "FastSLAM 2.0," *FastSLAM: A scalable method for the simultaneous localization and mapping problem in robotics*, pp. 63–90, 2007.

[19] Clifford, "Preliminary sketch of biquaternions," *Proceedings of the London Mathematical Society*, vol. s1-4, no. 1, pp. 381–395, 1871.

[20] B. Kenwright, "A beginners guide to dual-quaternions: what they are, how they work, and how to use them for 3D," in *The 20th International Conference in Central Europe on Computer Graphics, Visualization and Computer Vision, WSCG 2012 Conference Proceedings*, 2012, pp. 1–13.

[21] W. R. Hamilton, "Ii. on quaternions; or on a new system of imaginaries in algebra," *Philosophical Magazine Series 3*, vol. 25, no. 163, pp. 10–13, 1844.

[22] I. Gilitschenski, G. Kurz, and U. D. Hanebeck, "A stochastic filter for planar rigid-body motions," in *2015 IEEE International Conference on Multisensor Fusion and Integration for Intelligent Systems (MFI)*. IEEE, 2015, pp. 13–18.

[23] C. Bingham, "An antipodally symmetric distribution on the sphere," *The Annals of Statistics*, pp. 1201–1225, 1974.

[24] G. Kurz, I. Gilitschenski, F. Pfaff, and L. Drude, "libDirectional," 2015. [Online]. Available: https://github.com/libDirectional

[25] B. Ristic, S. Arulampalam, and N. Gordon, *Beyond the Kalman filter: Particle filters for tracking applications*. Artech house, 2003.

[26] J. Steinbring, "Nonlinear Estimation Toolbox," 2015. [Online]. Available: https://bitbucket.org/nonlinearestimation/toolbox